

2

AD-A174 962

Report No. R86-956939-2
Date: 12 September 1986
Prepared by: F. O. Carta
P. F. Lorber

Dynamic Stall Penetration Experiments on a Swept Wing

Annual Technical Report No R86-956939-2
Period Ending 15 August 1986
Contract F49620-84-C-0082

DTIC
SELECTED
S D
DEC 10 1986
D

1. The objective of this program is to determine the aerodynamic response of a model wing to large amplitude pitching motions under stalled and unstalled conditions. A wing section instrumented with 72 pressure transducers and 8 surface hot film gages has been constructed. The model was tested at 49 different conditions. Each condition consisted of an oscillatory or constant pitch rate ramp motion at a Mach number of 0.2, 0.3, or 0.4. The pitch angle was varied in the region between 0 and 30 deg by a hydraulic drive system. A computer controlled data acquisition system was used to sample, record, and process the data. The on-line data processing included computing the ensemble average of the pressure and heat transfer signals, computing the rms of the variation about this ensemble, converting the results to pressure coefficient, and integrating the pressure results to determine the steady and unsteady normal force and pitching moment coefficients. The ensemble average, rms, and raw pressure and hot film data are being examined to determine the variations in time and space of the transition and separation locations. Analysis of the ramp data will emphasize the influence of pitch rate, initial and final angles of attack, and Mach number. The oscillatory data are being analyzed similarly, emphasizing the related parameters of reduced frequency, mean angle, oscillation amplitude, and Mach number. Comparisons are being made between the two types of motion.

2. The second year of this contract has been devoted to completing fabrication of the instrumented model for the tunnel spanning (two-dimensional) portion of the experiment, and conducting experiments at 0 sweep angle. The wing had a span of 8 feet and a chord of 17.3 inches. It was tested in the UTRC Main Wind Tunnel at free stream Mach numbers of 0.2, 0.3, and 0.4, with equivalent Reynolds numbers based on chord of approximately 2×10^6 , 3×10^6 , and 4×10^6 , respectively. These values are an order of magnitude greater than the so-called critical Reynolds number of 3×10^5 and the results obtained in this experiment can be expected to be relevant to the problems of full scale aircraft. In the text that follows these introductory comments, some of the results obtained will be discussed and examined, based on a set of figures which, at present, are necessarily preliminary. Nevertheless, the general observations of this document are believed to be fundamentally correct. They are self consistent, and appear to have rational explanations.

DTIC FILE COPY

DISTRIBUTION STATEMENT A
Approved for public release;
Distribution Unlimited

86 12 09 047

REPORT DOCUMENTATION PAGE

1a. REPORT SECURITY CLASSIFICATION Unclassified		1b. RESTRICTIVE MARKINGS --	
2a. SECURITY CLASSIFICATION AUTHORITY		3. DISTRIBUTION / AVAILABILITY OF REPORT unlimited	
2b. DECLASSIFICATION / DOWNGRADING SCHEDULE			
4. PERFORMING ORGANIZATION REPORT NUMBER(S) R86-956939-2		5. MONITORING ORGANIZATION REPORT NUMBER(S) AFOSR-TR- 86-2209	
6a. NAME OF PERFORMING ORGANIZATION United Technologies Research Center	6b. OFFICE SYMBOL (if applicable) --	7a. NAME OF MONITORING ORGANIZATION AFOSR/DA	
6c. ADDRESS (City, State, and ZIP Code) Silver Lane East Hartford, CT 06108		7b. ADDRESS (City, State, and ZIP Code) Building 410 Bolling AFB, DC 20332	
8a. NAME OF FUNDING / SPONSORING ORGANIZATION AFOSR	8b. OFFICE SYMBOL (if applicable) AFOSR/DA	9. PROCUREMENT INSTRUMENT IDENTIFICATION NUMBER F49620-84-C-0082	
8c. ADDRESS (City, State, and ZIP Code) AFOSR/ Bolling AFB, DC 20332		10. SOURCE OF FUNDING NUMBERS	
		PROGRAM ELEMENT NO. 61102F	PROJECT NO. 2307
		TASK NO. A1	WORK UNIT ACCESSION NO.
11. TITLE (Include Security Classification) Dynamic Stall Penetration Experiments on a Swept Wing - Second Annual Report			
12. PERSONAL AUTHOR(S) Carta, Franklin O.; Lorber, Peter F.			
13a. TYPE OF REPORT Annual	13b. TIME COVERED FROM 8/15/85 to 8/15/86	14. DATE OF REPORT (Year, Month, Day) 1986, Sept. 12	15. PAGE COUNT 21
16. SUPPLEMENTARY NOTATION			
17. COSATI CODES		18. SUBJECT TERMS (Continue on reverse if necessary and identify by block number)	
FIELD	GROUP	SUB-GROUP	
		Unsteady Aerodynamics; Dynamic Stall; Aerodynamic Testing; Unsteady Measurement Techniques.	
19. ABSTRACT (Continue on reverse if necessary and identify by block number)			
<p>➤ An experiment was conducted to study the aerodynamic response of a wing to large amplitude pitching motions, including dynamic stall. A two-dimensional model was tested at Mach numbers of 0.2, 0.3, and 0.4, corresponding to Reynolds numbers between 2×10^6 and 4×10^6. A total of 49 unsteady conditions were studied, including both sinusoidal oscillations and constant pitch rate ramps. The ramp motions ranged up to 0 to 30 deg at pitch rates between 17.5 and 350 deg/sec. A preliminary analysis of the results shows significant effects of pitch rate and Mach number on the surface pressures, integrated airloads, and locations of boundary layer transition and separation. A pressure oscillation was detected in the post stall region that appears to result from periodic vortex shedding that has synchronized to the imposed pitching motion. A more detailed analysis of these results will be conducted during the remainder of this activity.</p>			
20. DISTRIBUTION / AVAILABILITY OF ABSTRACT <input checked="" type="checkbox"/> UNCLASSIFIED/UNLIMITED <input type="checkbox"/> SAME AS RPT. <input type="checkbox"/> DTIC USERS		21. ABSTRACT SECURITY CLASSIFICATION	
22a. NAME OF RESPONSIBLE INDIVIDUAL DR JAMES D WILSON		22b. TELEPHONE (Include Area Code) 802-707-4935	22c. OFFICE SYMBOL AFOSR/DA

The experiment consisted of several phases, starting with a basic steady state measurement of pressures, using the miniature transducers as the source of the data, corroborated by auxiliary pneumatic pressure ports. The bulk of the unsteady data were taken during constant pitch rate excursions, or ramps. Most were positive ramps, with angle of attack varying from low to high values, but a few were negative ramps. In addition, a selected set of sinusoids were also taken to compare with the large body of sinusoidal data already available in the literature. In all of these unsteady runs the data were obtained from the same set of miniature high-response transducers. On-line monitoring of the individual and integrated outputs permitted value judgements to be made of the viability of the instrumentation and of the validity of the resulting data. The steady and unsteady conditions run during the experiment are summarized and tabulated in Table 1. There were a total of 2 steady runs, 40 ramps, and 9 sinusoids.

Hot Film Correlations with Pressures

Correlation between hot film and pressure rms is very important. Both responses are dominated by strong time-dependent signatures that overwhelm the random, unsteady responses associated with turbulence or separation. In the case of the hot film, this signature clearly defines the three flow regimes (i.e., laminar, turbulent, separated). However, the pressure signature is dominated by the gross change in load up to the suction peak, followed by the collapse of suction in the stall. These changes are very large compared with the pressure response to turbulence, and mask all random pressure responses except for large changes caused by separation. Hence, little flow regime information is available from raw pressure time histories.

Generally, the information sought by the experiment is driven by the application requirements, and hence the load information from pressure transducers takes precedence over hot film data. It is further driven by the relative ease of acquiring data from pressure transducers, and the more difficult task of obtaining hot film data from temperamental circuits. In the past this has meant that surface flow details would be lost except for the few locations where hot films were placed. The theoretician attempting to use these data for code verification would have very little data to judge his predictive capabilities.

In the present experiment we have sought to remedy this by removing the repetitive time-dependent signature from both pressure and hot film responses. This is done by on-line ensemble-averaging all repetitive time histories and also forming the rms of the variation about the ensemble average of each individual cycle (or ramp) of the motion. This is done for both sets of data (i.e., pressures and hot films). A limited sampling of the two shows a strong correlation between the hot film rms and pressure rms from neighboring surface stations such that the onset of transition and of separation is clearly signalled by both rms responses at the same dimensionless time. (The actual events are confirmed by examination of the full hot film time history.) Thus, it is now possible (in principle) to use this concept to map the space-time coordinates of transition and separation from the traditional instrumentation array of many pressure transducers and few hot film gages.

for	
&I	<input checked="" type="checkbox"/>
d	<input type="checkbox"/>
	<input type="checkbox"/>
Activity Codes	
and/or Special	

A-1

This brief report shows this correlation for a pair of stations on the suction surface of the airfoil. A more detailed examination will be provided in the final report, although even here, the results will be somewhat limited by the two-dimensionality of the experimental geometry (i.e., full span, unswept wing). If the results of our detailed study confirm this technique to be both viable and consistent, the next obvious step is to proceed with the free tip experiment to study 3-D effects, and to look at the effects of sweep on these results. Such a data set will be invaluable to theoreticians involved in code development, and to designers seeking transient load information.

Aircraft Stability in Stall Penetration Maneuvers

Many of the parameters chosen for this experiment were sized by their applicability to the problem of deep stall penetration of a maneuvering aircraft. One of the more obvious requirements for such a flight condition is that the aircraft remain in stable flight, either passively, as in normal flight, or dynamically, through active controls. Either way, it is imperative that the flow dynamics and the associated wing response be known or predictable through stall penetration and beyond.

The results examined to date from this experiment (and sampled in this document) show that the post stall behavior of a wing penetrating stall at constant pitch rate is anything but steady. This is not surprising in view of previous studies of sinusoidal motions which showed traditional stall flow breakdown after an overshoot of lift and moment beyond the quasi-steady stall point. This has also been observed in the few constant pitch rate stall penetrations reported in the literature. However, the behavior of the post stall flow observed in this experiment appears to have significant differences from most of these previous results. (This may be related to the order of magnitude increase in Reynolds number in the present experiment relative to that of most earlier work.) In general, once stall has occurred, the individual pressure traces for both suction and pressure surfaces appear to respond almost sinusoidally with time. The regular period of the response on the suction surface is surprising because the flow is ostensibly separated, with a free streamline between the separated region and the blade. At an angle of 30 deg, this should be a considerable distance from the airfoil surface, and the mechanism to cause a coherent response from the several points on the airfoil surface is not readily apparent. However, it may be a result of Karman-like vortex shedding, best explained on the basis of the unseparated pressure surface flow.

The coherent response on the pressure surface is not so surprising if one looks at the airfoil at large angle of attack as a bluff body shedding vorticity. Assuming that a Karman street behavior is possible, one would expect a periodic shedding from the sharp trailing edge to cause periodic changes in the trailing edge pressure, with a consequent change in the potential field of the entire pressure surface. This is demonstrated in the sample results included in this document, and a rough calculation of the shedding frequency, based on the bluff body presented to the flow, is within a factor of 2 of the measured frequency. If this is a reasonable

explanation, then the periodic change in pressure at the trailing edge may also cause a periodic response to occur over the separated suction surface as well. A detailed analysis of the results is beyond the scope of this document, and the phenomenon will be studied in more detail as part of the data analysis and final report phase of the work.

Whatever the reason behind the observed response, it is evident that it is a real effect, and the overall correlation of the response from point to point on the two surfaces lends credence to the observations. It will be shown that the lift and moment responses are comparably affected, and exhibit large oscillatory changes also. Hence, any aircraft involved in a deep stall maneuver could be subjected to large oscillations, and any requirement for a stable attitude during maneuver could be severely compromised if a sufficient body of information is not provided to the designer of the control systems.

Selected Experimental Results

The first phase of this experiment was composed of a total of 49 steady and unsteady runs that measured the surface pressures and hot film responses on a tunnel-spanning (two-dimensional) wing model mounted at 0 sweep. The runs are listed in Table 1. The ramp motion was composed of an initial period of constant angle (for 1/8 of the cycle), a period of constant (either positive or negative) pitch rate (for 1/2 of the cycle), and a final period of constant angle (for 3/8 of the cycle). The ensemble average and root-mean-square variation about this average were computed based upon 20 cycles.

Ensemble averaged suction surface pressures for a 0 to 30 deg ramp at $M=0.2$ and a pitch rate $A=c\dot{\alpha}/2U=.005$ (87.5 deg/sec) are shown in Fig. 1. The labels used for the pressure transducers are defined in Table 2. The pressure time histories are characterized by a constant initial value, followed by a nearly linear increase as the angle of attack increases up to the time of dynamic stall. At this time the suction peak pressure collapses rapidly. The pressure disturbance created by the downstream convection of the stall vortex occurs at successively later times at transducers located further downstream on the airfoil chord. The ensemble averaged pressures in the fully separated region approach values that are nearly constant both in time and space. Figure 2 shows the pressure surface pressures for the same conditions at the same chordwise locations. The pressures are again nearly constant during the initial period. As the angle of attack increases the stagnation point (where C_p is near +1.0) moves downstream on the pressure surface, past the $x/c=.005$ transducer (S1) and stops near the $x/c=.0256$ transducer (S2). Following stall the pressures are a combination of a fundamentally constant pressure and a 58 hz oscillation. Note that this is not a 60 Hz electrical noise problem, since the oscillations only occur in stalled flow. A probable explanation is a periodic vortex shedding that has synchronized with the airfoil motion, so that it is not only observed in the unaveraged pressure traces, but also in the ensemble average.

Figures 3 and 4 show surface pressure results for the high pitch rate case of $A=.02$ (350 deg/sec), with all other conditions identical to Figs. 1 and 2. The primary changes are an increased suction peak pressure and a much larger oscillatory pressure on both surfaces after stall. The frequency of

the oscillation has changed to approximately 48 Hz. The oscillation is also present when the pressures are integrated to obtain the lift and moment coefficients per-unit-span. The lift curve (Fig. 5) shows a linear region for lower angles of attack, an increase in the lift slope by a factor of 2.4 just prior to stall, a rapid stall, and the vortex-induced oscillation after stall. The curve of the pitching moment about the quarter-chord (positive nose up) in Fig. 6 shows a very sharp drop at stall, followed by the post-stall oscillation.

There are many qualitative similarities between the constant pitch-rate ramps and sinusoidal oscillations. This is shown by the pressure time histories for $\alpha = 20 + 10\sin\omega t$, at a reduced frequency $k = c\omega/2U = .50$ (Figs. 7 and 8). Again there is a rapid stall on the suction surface, downstream convection of the stall vortex, a region of constant stalled pressure on the suction surface, and a final reattachment. The post-stall oscillations are again present, this time at a frequency of 56 Hz, approximately 23 times the airfoil pitching frequency. The maximum amplitude of the oscillation occurs near the trailing edge. This is consistent with a disturbance to the external potential flow that results from periodic vortex shedding from the trailing edge.

The use of ensemble averaged and rms variations to deduce surface conditions is illustrated in Fig. 9. Figure 9a shows the time history of the ensemble averaged pressure at $x/c = .0256$ for the conditions of Fig. 3. Separation occurs at a nondimensional time of 0.56 at this position. Figure 9b shows the ensemble averaged skin friction gage voltage at the same chordwise location. The heat transfer is constant over the initial period, and then decreases as the angle of attack increases and the laminar boundary layer thickens. The sharp increases in heat transfer between $t = .38$ and $.44$ results from transition to turbulence. This is followed by a decrease in heat transfer as the turbulent layer thickens. Separation is indicated at $t = .56$ by an increased roughness in the time history and a much shallower rate of decrease in the heat transfer with time. The rms of the skin friction gage output voltage (Fig. 9c) is very low when the boundary layer is laminar, and has a sharp increase at the beginning of transition ($t = .38$). There is a second increase at separation ($t = .56$), followed by a high rms level during the entire period of separated flow. The rms of the pressure (Fig. 9d) is also initially near zero, and increases by a small, but noticeable amount at $t = .33$, just prior to the time when the onset of transition is indicated by the skin friction gage. A further massive increase in the pressure rms occurs at separation ($t = .54$). The good correlation between the pressure and heat transfer results shown is typical of the other cases examined to date. The time of separation was always in agreement, and, although there were some differences in indicated times of transition, the combined use of ensemble averaged and rms quantities should be useful in determining surface flow conditions.

3. The original plan for this research assumed that the hydraulic drive and support system would be designed, fabricated, fitted to the wind tunnel, and checked out in advance of the start of this program. Funding for this work was to be covered by the Sikorsky Aircraft Division in connection with their planned entry into the wind tunnel to perform similar unsteady testing. Unfortunately the Sikorsky wind tunnel program was cancelled. Therefore, full Sikorsky support was not available, nor did they supply the spar required to perform the finite tip portion of the

test. Consequently it was necessary to use contract funds to complete the installation of the drive and support system in the wind tunnel. The design, fabrication, and checkout of the hydraulics was still covered by Sikorsky. This reduced the total number of experimental tasks that could be completed with the available time and funding. Furthermore, it was necessary to defer the finite-tip portion of the program. The contract technical monitor has been apprised of these circumstances in a number of telephone conversations in August and September 1986, and a meeting is planned at AFOSR in late September to discuss this program in detail.

4. The professional personnel directly associated with this research activity are:

Mr. Franklin O. Carta (Principal Investigator)
Dr. Peter F. Lorber

Additional professional personnel involved in the design and fabrication of the model and associated electronics, and in the operation of the experiment, included:

Dr. Larry W. Hardin
Mr. Joseph P. Haley
Mr. John E. Ayer
Mr. Arthur W. Simmonds

TABLE 1

STEADY

$$M = 0.2, \quad -5^\circ \leq \alpha \leq 28^\circ$$

$$M = 0.4, \quad 0^\circ \leq \alpha \leq 20^\circ$$

UNSTEADY RAMPS

$$A = C\dot{\alpha}/2U$$

M	α -RANGE	.001	.0025	.005	.010	.020
0.2	$0^\circ \rightarrow 10^\circ$	x	x	x	x	
	$0^\circ \rightarrow 20^\circ$	x	x	x	x	
	$0^\circ \rightarrow 30^\circ$	x	x	x	x	x
	$10^\circ \rightarrow 20^\circ$	x	x	x	x	
	$12^\circ \rightarrow 22^\circ$	x		x	x	
	$14^\circ \rightarrow 24^\circ$	x		x	x	
	$20^\circ \rightarrow 30^\circ$	x	x	x	x	
	$20^\circ \rightarrow 10^\circ$	x			x	
	$30^\circ \rightarrow 0^\circ$	x		x		
0.3	$0^\circ \rightarrow 20^\circ$			x		
	$0^\circ \rightarrow 30^\circ$				x	
0.4	$0^\circ \rightarrow 10^\circ$	x		x		
	$0^\circ \rightarrow 20^\circ$	x	x	x	x	
	$20^\circ \rightarrow 0^\circ$				x	

(40 RAMPS)

UNSTEADY OSCILLATIONS

$$k = C\omega/2U$$

M	α	.025	.050	.100
0.2	$5^\circ + 5^\circ \sin \omega t$	x		
	$10^\circ + 10^\circ \sin \omega t$	x	x	x
	$20^\circ + 10^\circ \sin \omega t$	x	x	x
0.3	$9^\circ + 8^\circ \sin \omega t$		x	
	$12^\circ + 8^\circ \sin \omega t$			x

(9 SINUSOIDS)

TABLE 2

PRESSURE TRANSDUCER & HOT FILM LOCATIONS

STATION 4:		PRESSURE TRANSDUCERS		HOT FILMS
#	x/c	SUCTION SURFACE	PRESSURE SURFACE	
1	.0050	CPK04S1	CPK04P1	
2	.0256	" S2	" P2	SFG06S1
3	.0597	" S3	" P3	" S2
4	.1028	" S4	" P4	" S3
5	.1490	" S5	" P5	
6	.1920	" S6	" P6	" S4
7	.2262	" S7	" P7	
8	.2468	" S8	" P8	
9	.2616	" S9	" P9	
10	.3023	" S10	" P10	" S5
11	.3718	" S11	" P11	
12	.4638	" S12	" P12	" S6
13	.5702	" S13	" P13	
14	.6816	" S14	" P14	" S7
15	.7880	" S15	" P15	
16	.8800	" S16	" P16	" S8
17	.9495	" S17	" P17	
18	.9902	" S18	" P18	

FIGURE 2 PRESSURE SURFACE PRESSURES

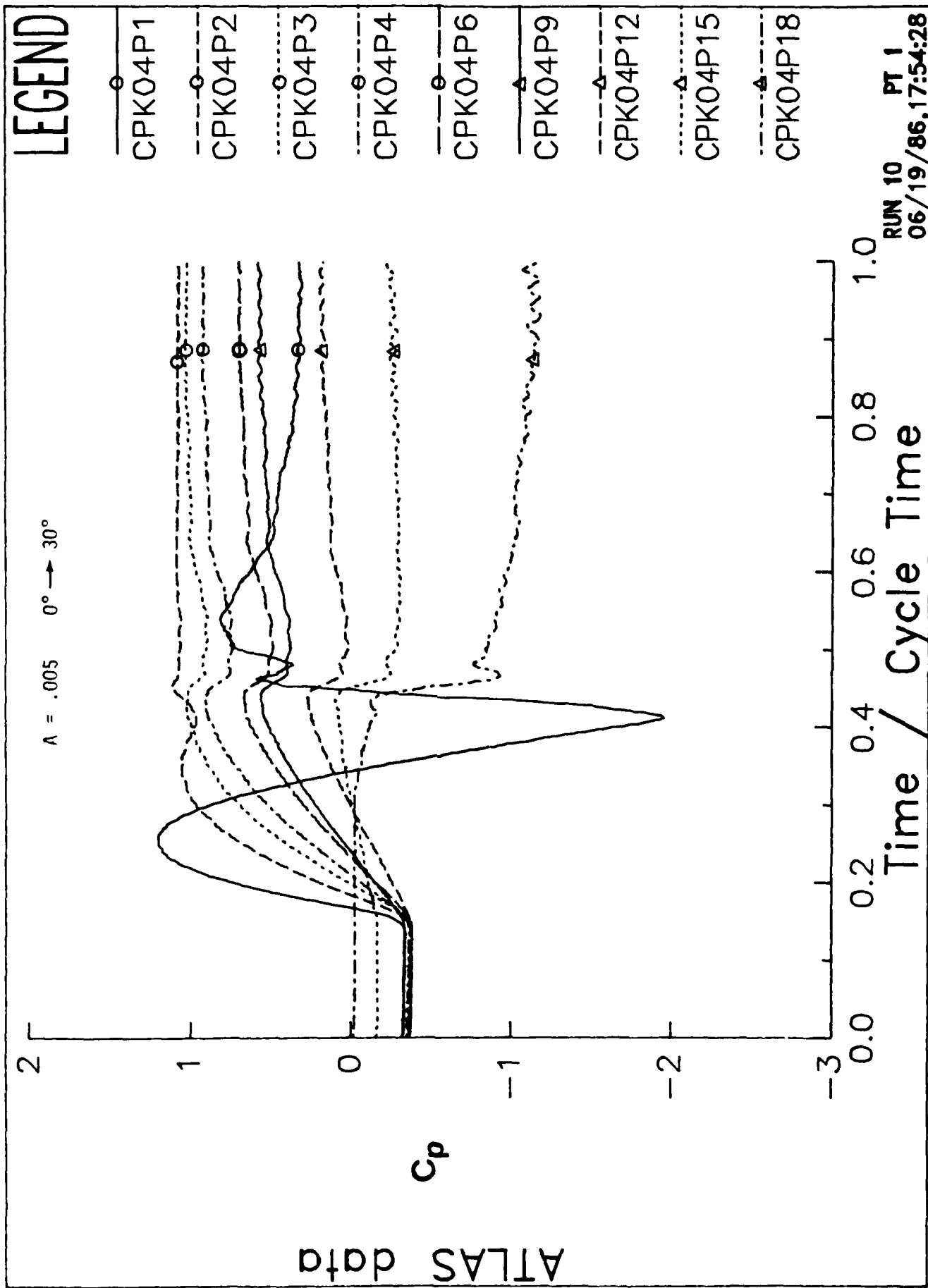


FIGURE 3 SUCTION SURFACE PRESSURES

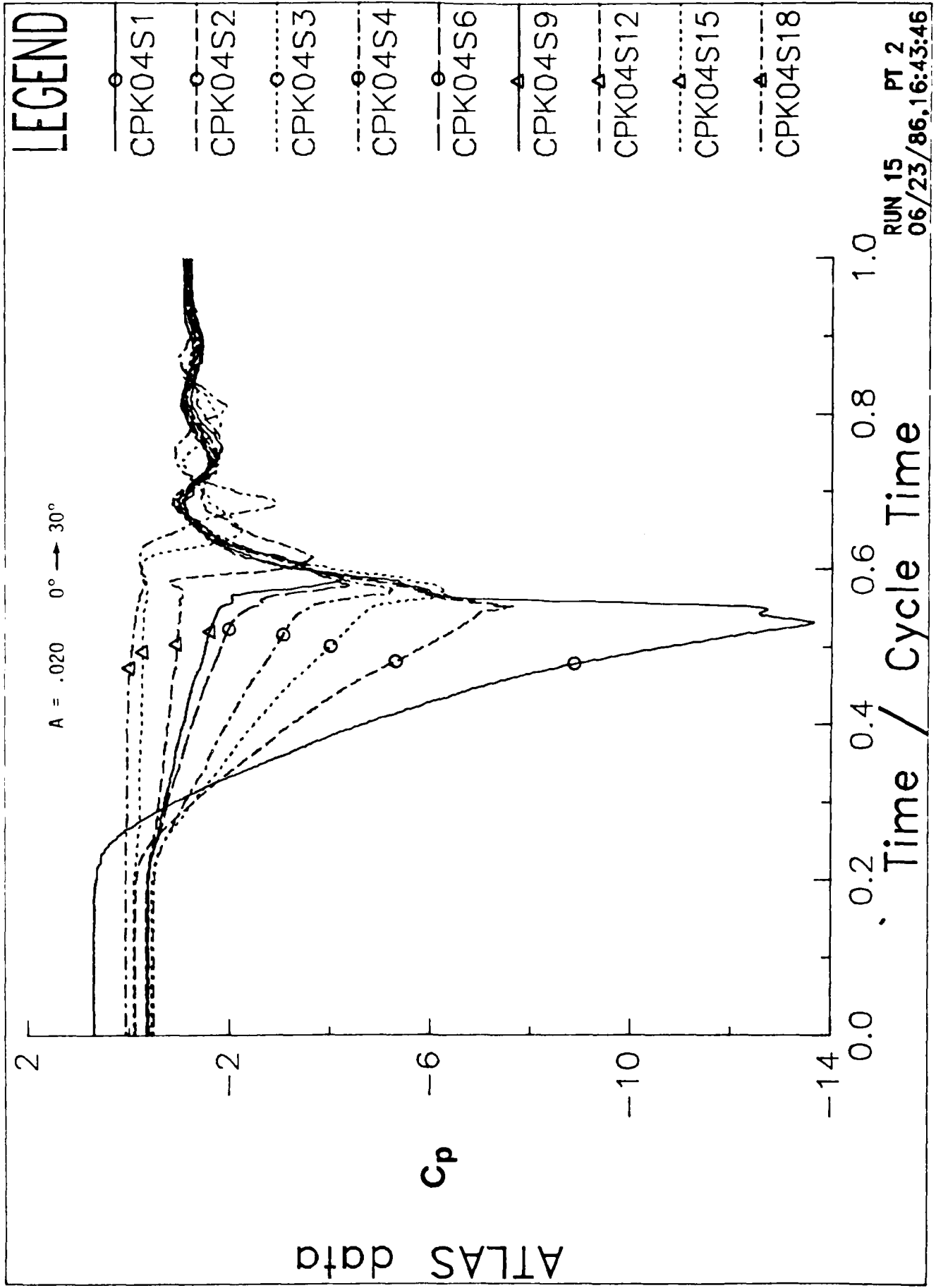


FIGURE 4 PRESSURE SURFACE PRESSURES

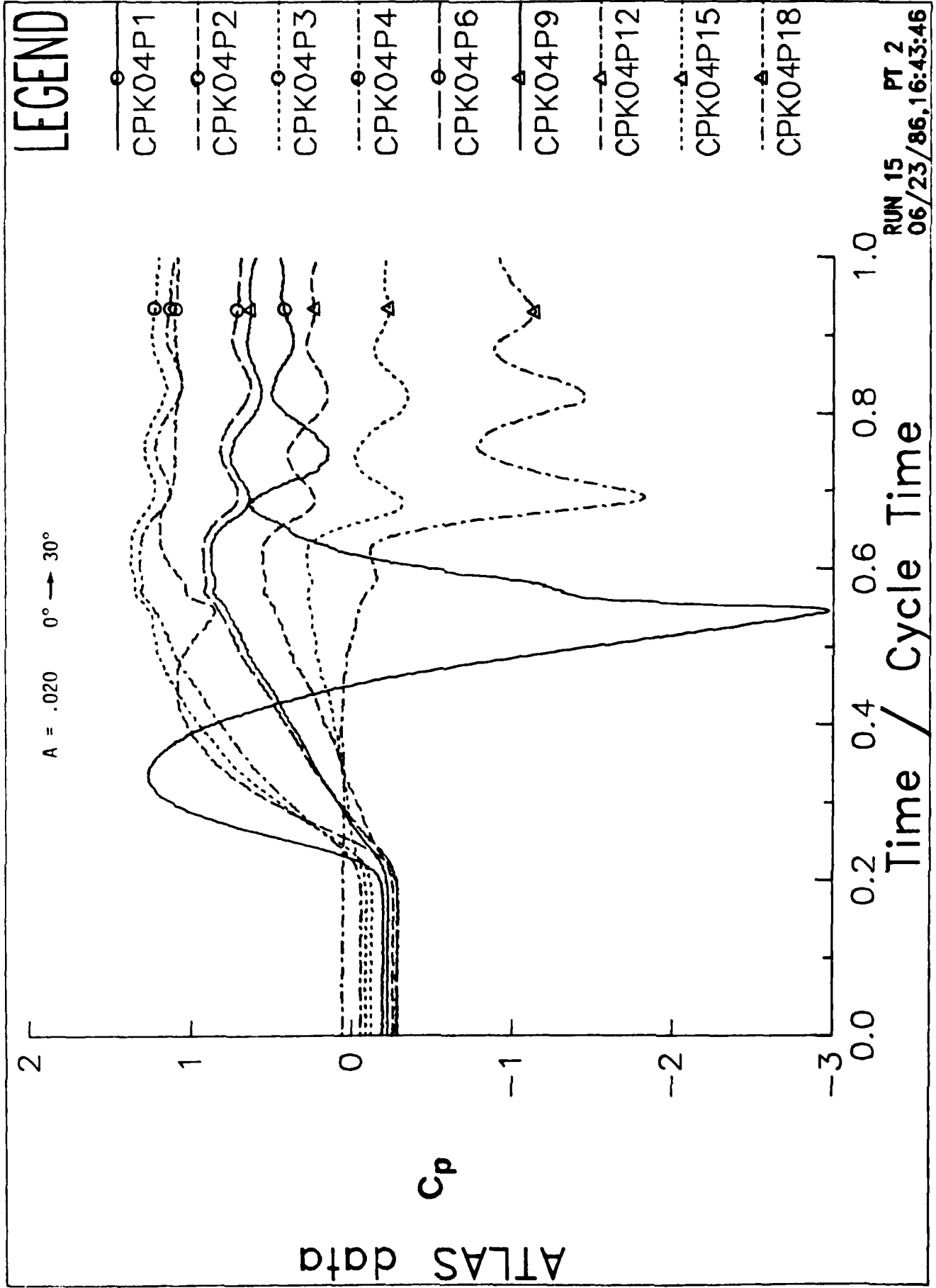


FIGURE 5 LIFT

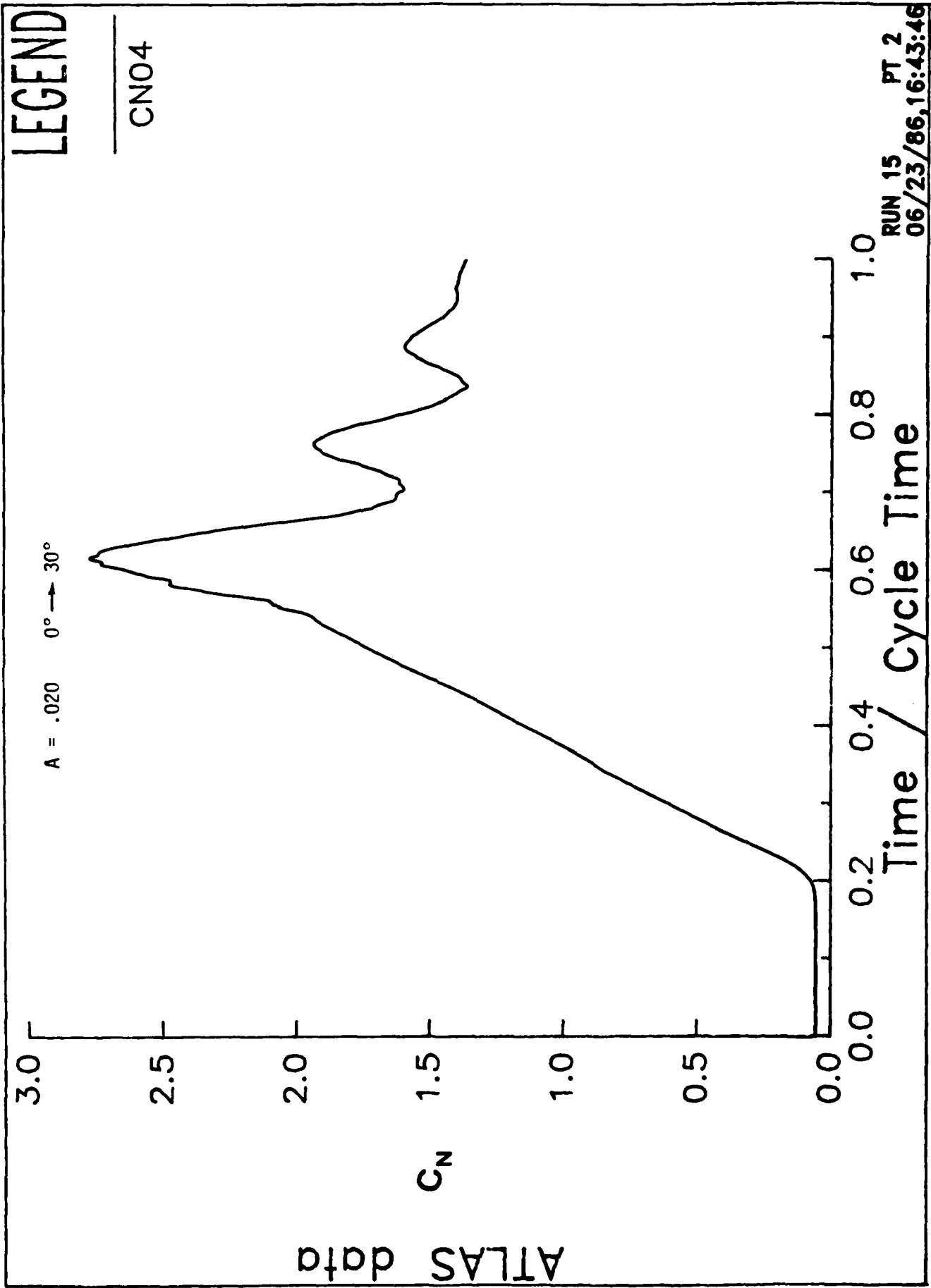


FIGURE 6 PITCHING MOMENT

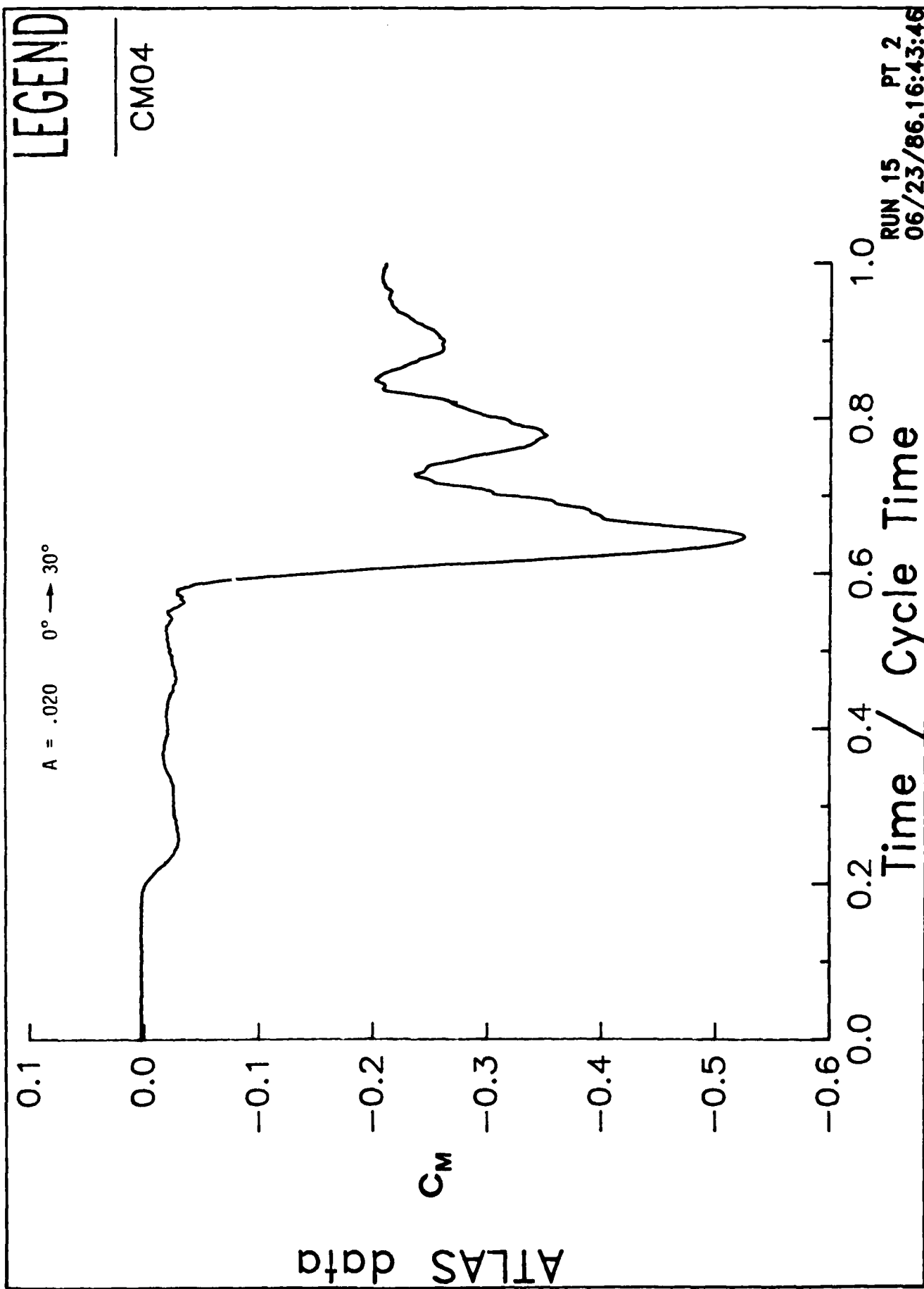


FIGURE 7 SUCTION SURFACE PRESSURES

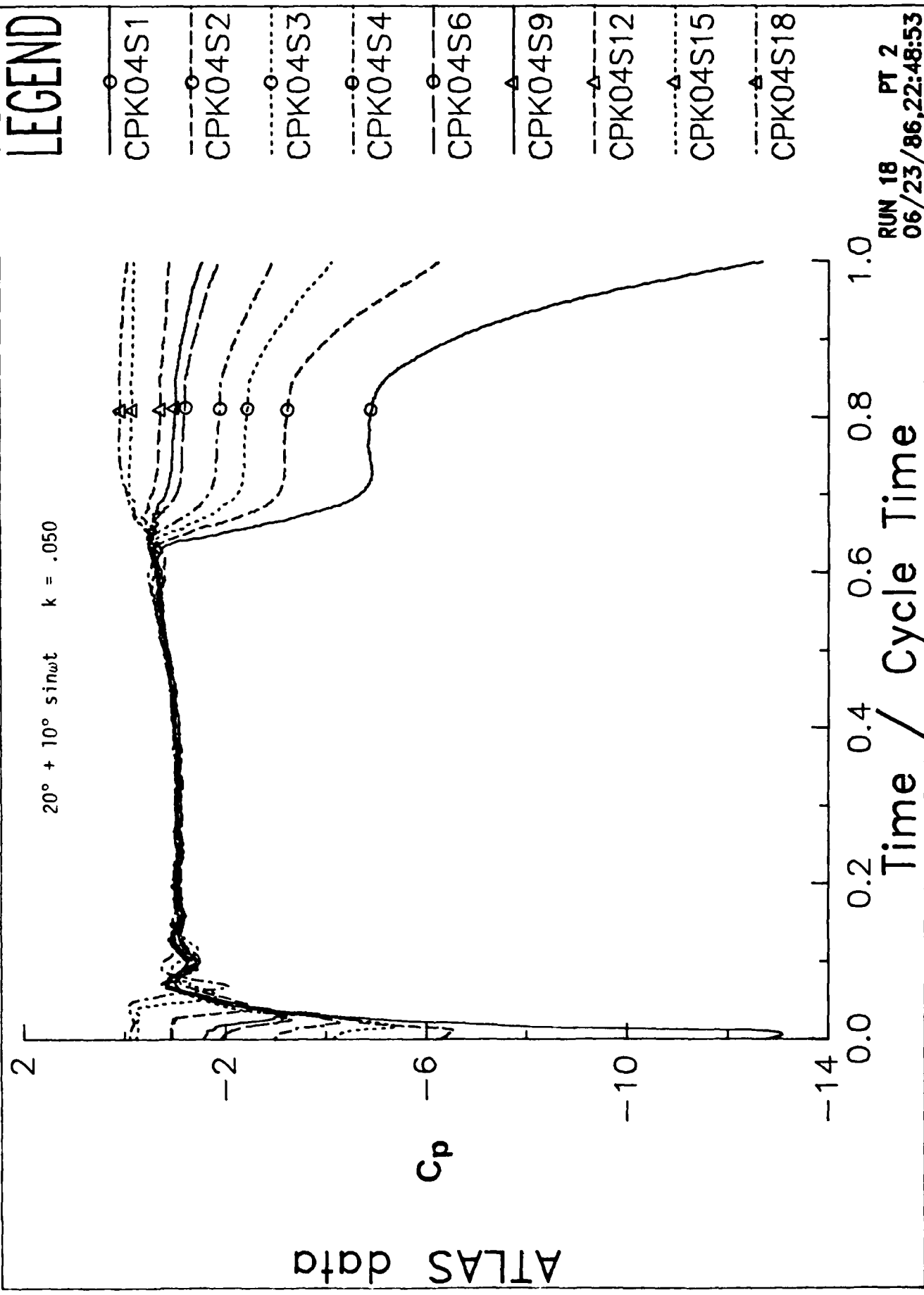


FIGURE 8 PRESSURE SURFACE PRESSURES

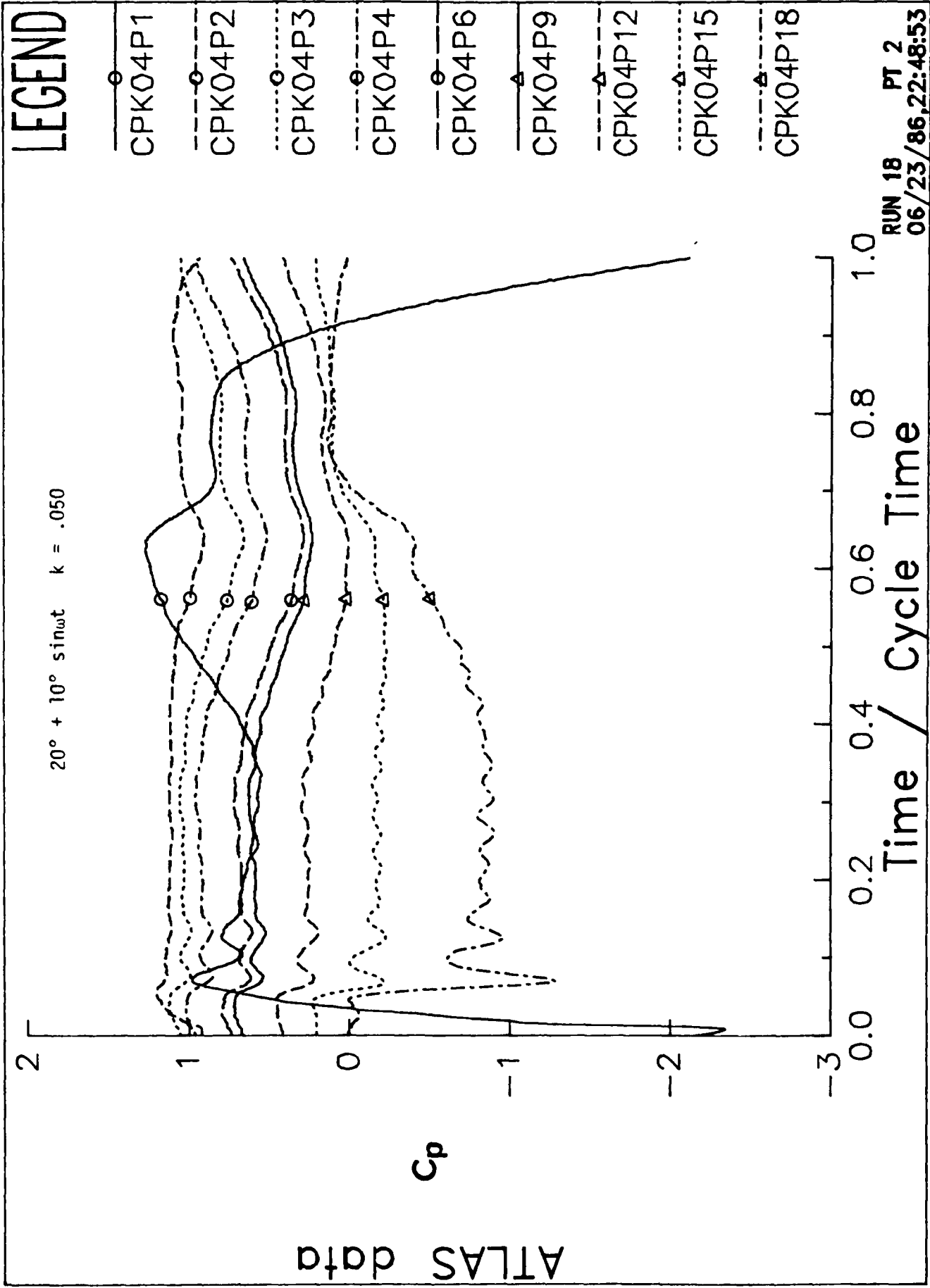


FIGURE 9a ENSEMBLE-AVERAGED PRESSURE COEFFICIENT

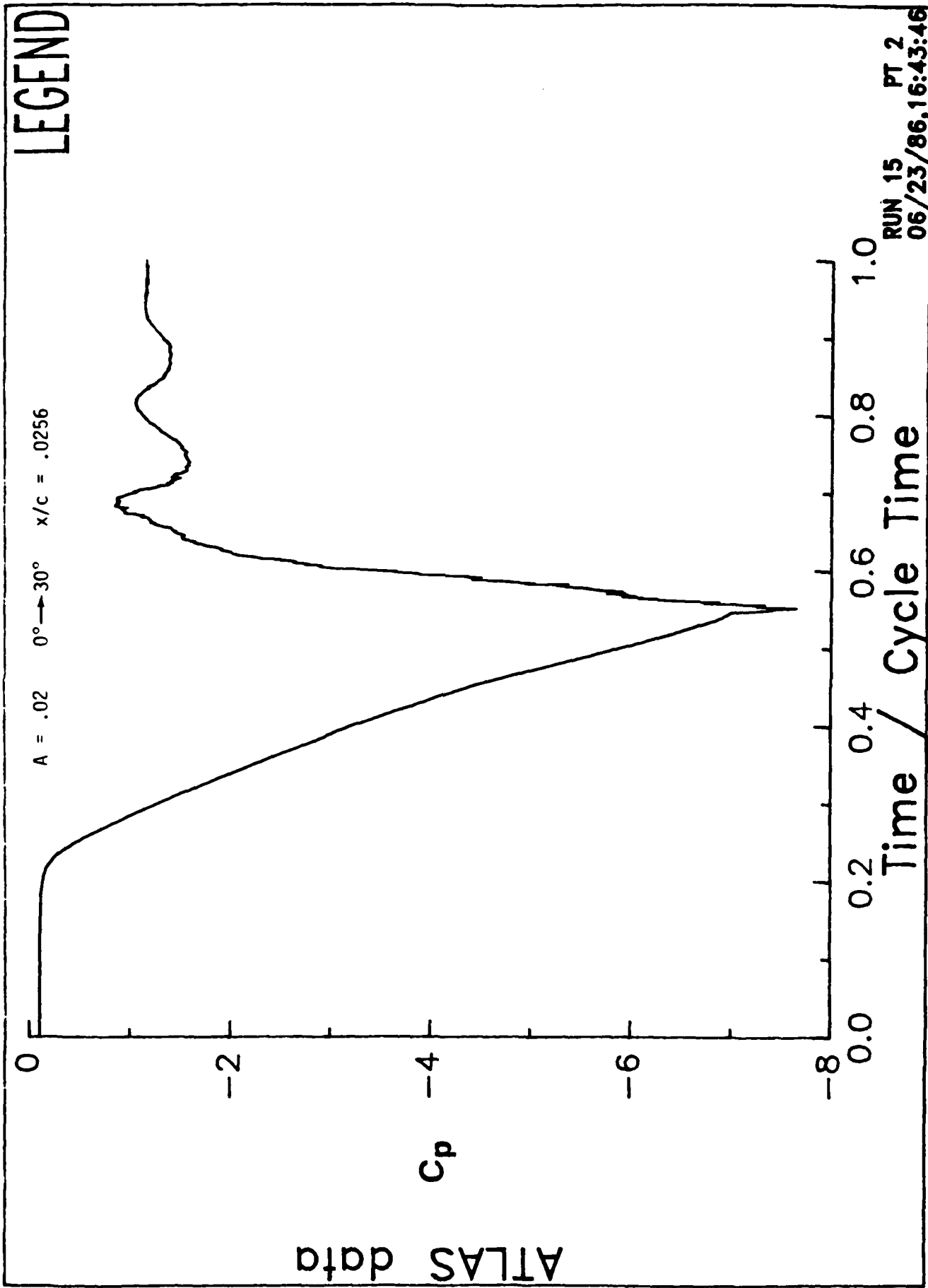


FIGURE 9b ENSEMBLE-AVERAGED HEAT TRANSFER

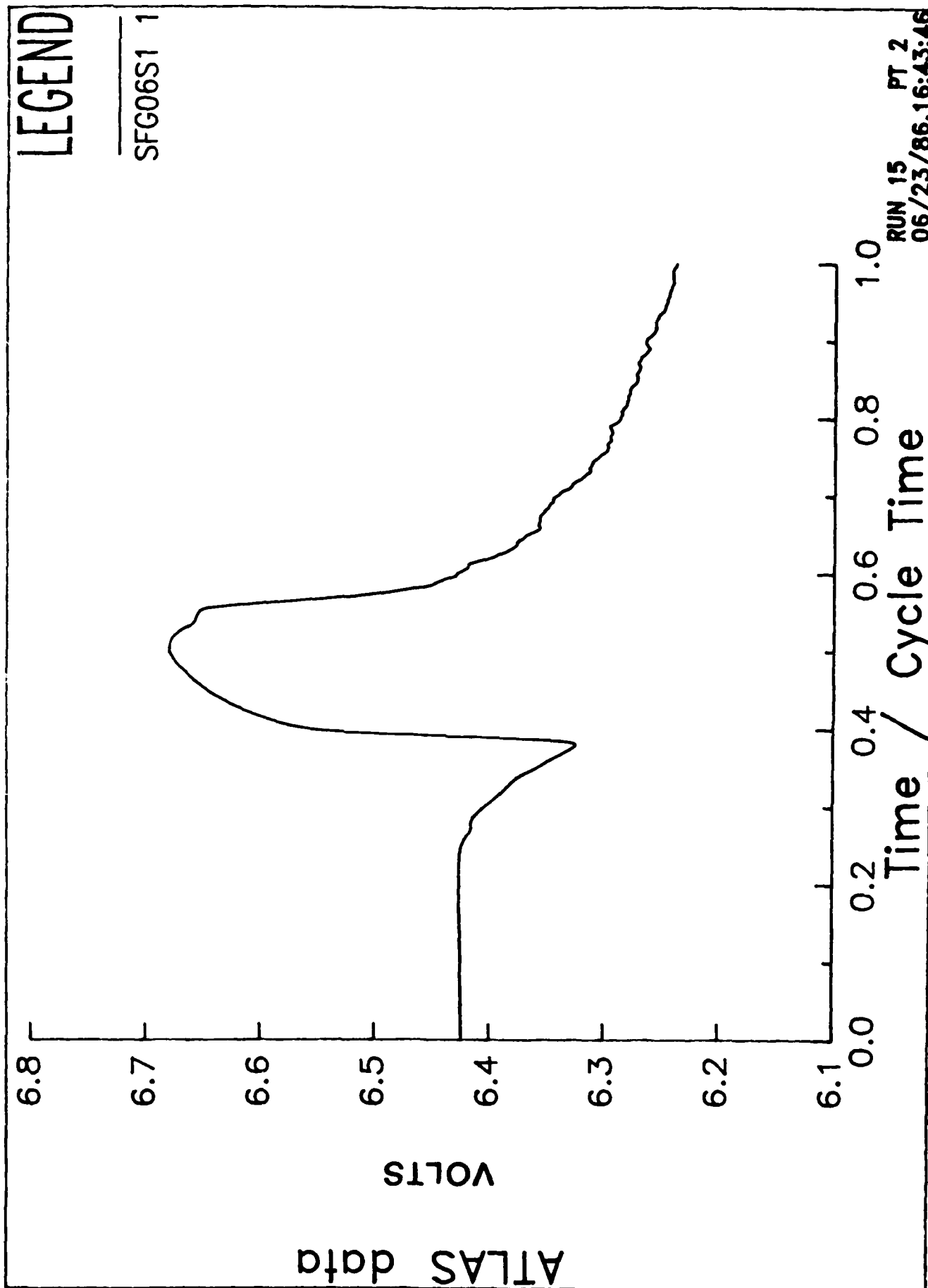


FIGURE 9c R.M.S. HEAT TRANSFER

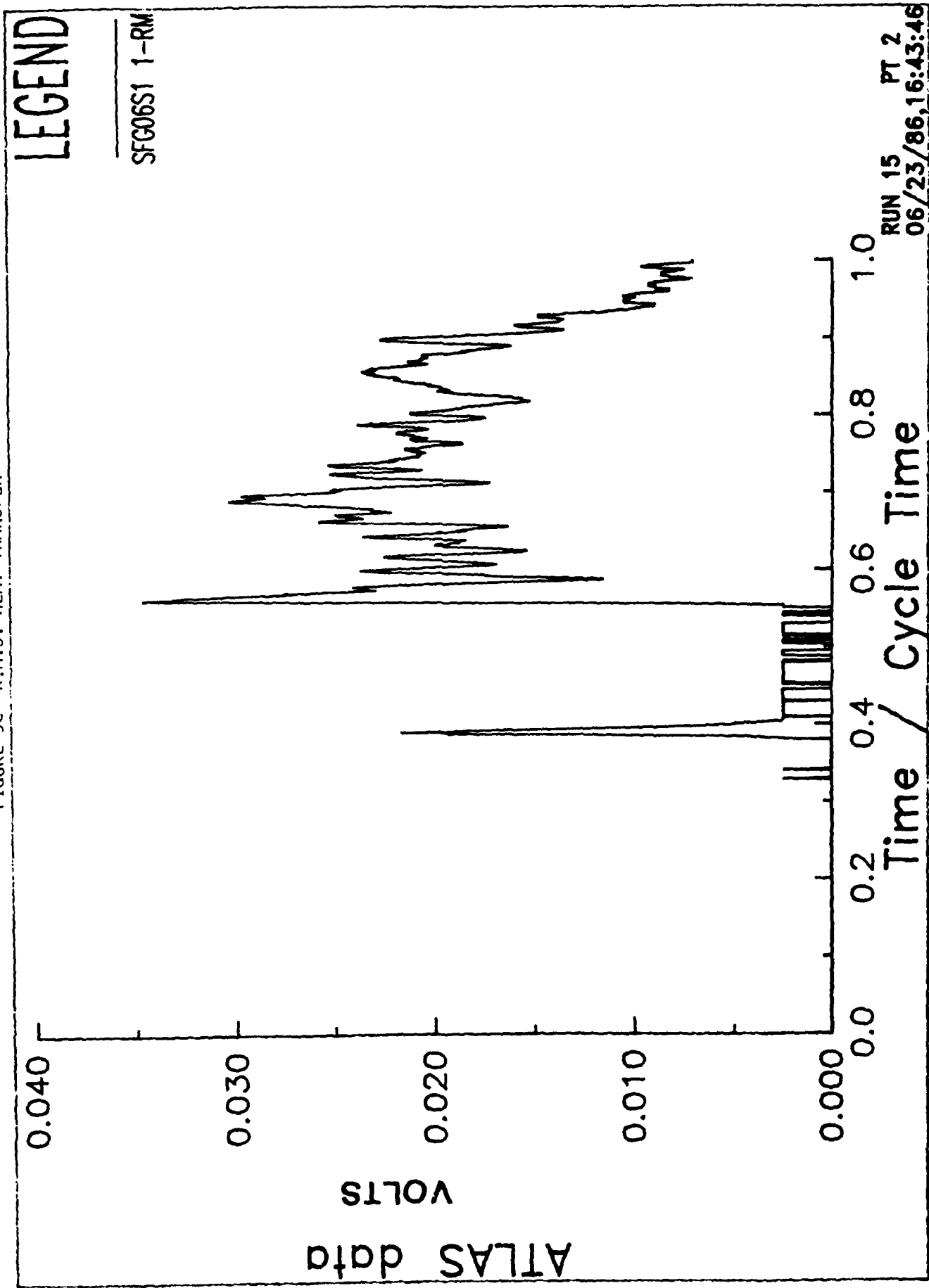


FIGURE 9d R.M.S. PRESSURE

